A Global Surface Albedo Model

JOHN R. HUMMEL AND RUTH A. RECK

Physics Department, General Motors Research Laboratories, Warren MI 48090

(Manuscript received 28 September 1978, in final form 21 November 1978)

ABSTRACT

We have shown in the past that the radiative-convective energy balance atmospheric model used at the General Motors Research Laboratories in our atmospheric physics research is extremely sensitive to the input value of surface albedo used. In response to this we developed a new global model of the surface albedo based on a detailed analysis of land use. The model has been used to determine the average surface albedo of the earth's surface in latitudinal bands for the four seasons of the year (January–March, April–June, July–September and October–December). In addition, global maps of surface albedo for elements 10° latitude by 10° longitude are provided. Our model involves assigning one of 49 different types of surface to each of 77 040 areas for each of the four seasons. Each type of surface is assigned a different albedo for each season. The average surface albedo for a given latitudinal band is obtained by averaging the albedos for the areas in the desired latitudinal band. The average surface albedos are intended to be used for input data in our radiative-convective energy balance model of the earth's atmosphere in order to compute the atmospheric temperature profile. The average annual albedo values for 18 different latitudinal bands are compared with the predictions of three other studies. The values in this work tend to be slightly lower than the others from 30°N–30°S and slightly higher from 90°–50°N and 50°–90°S. The annual global average albedo is calculated to be 15.40 as compared to 13.0 for the previous predictions.

1. Introduction

Our recent studies of the Manabe-Wetherald radiative-convective model for computing atmospheric temperature profiles indicate that the available input data for global surface albedo values with errors of $\pm 2.5\%$ (global albedo is $13.0 \pm 2.5\%$) produces an uncertainty of ± 2.5 K in the calculated surface temperature (Reck, 1978). The purpose of this present work was to reduce this uncertainty. The procedure we used was to develop a more accurate global surface albedo model by obtaining the most recent estimates of land usage and improved albedo measurements from the many types of earth surfaces. The model involves assigning one of 49 different types of surfaces to each of 77 040 areas for each quarter of the year, January–March, April–June, July–September and October–December. The purpose of this report is to describe how the earth's surface was segmented, how the 49 different types of surface were obtained and how the quarter-year-average albedos were obtained for each areal element.

For this study we define the surface albedo as the ratio of the wavelength-averaged solar radiation reflected by the earth's surface to that incident on it. In the literature one finds mention of two types of albedo—surface albedo and planetary albedo. The surface albedo is the solar reflectivity of a particular surface and is only a function of the radiation field incident on it and the properties of the surface itself. The planetary albedo, on the other hand, is the reflectivity of the entire earth–atmosphere system as viewed from space. In climatological studies of the heat balance of the earth the surface albedo is the desired quantity. [For a general discussion of how albedo varies with wavelength, angle of the sun, presence of clouds and age of vegetation see Bartman (1967), Kondratyev (1973), Idso *et al.* (1975), Paltridge and Platt (1976) and Lian and Cess (1977).]

Most surfaces are imperfectly diffuse reflectors. Water surfaces have a surface albedo that is highly dependent on the zenith angle of the sun. Soils and vegetative surfaces have albedos which vary much less with zenith angle. All surfaces have their clear-sky albedo minima at midday. Solar albedos for water surfaces exhibit very little wavelength dependence but vegetative areas exhibit highly wavelength-dependent albedos. Finally, the albedo of a surface is a function of cloud cover. The diffuse component due to solar reflection from clouds is added to the clear-sky albedos for unshaded surfaces. For small zenith angles, clouds tend to increase surface albedo for water and sand surfaces, while at large zenith angles clouds decrease the average surface albedo for their surfaces. Vegetative surfaces tend to have albedos which are independent of cloud cover. Therefore the clear-sky average albedos will not be greatly changed by clouds

0021-8952/79/030239-15$07.75

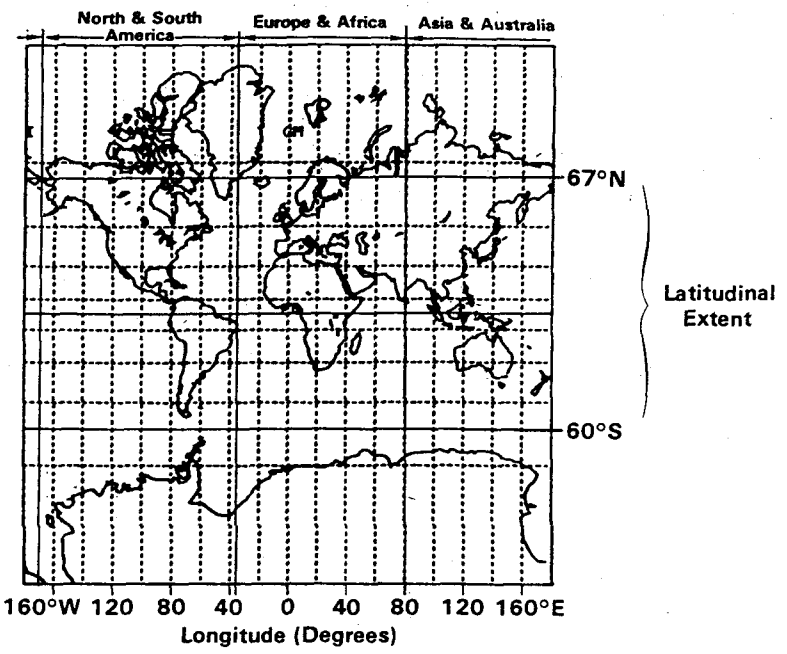

FIG. 1. Extent of data sets NSA, EAF and ASA.

when averaged over daylight hours. Nevertheless, considerably more work is needed in this area. All of the albedo values used in this work are based on direct measurements. Averages for the three month periods January–March, April–June, July–September and October–December are then employed to represent estimates of seasonal variations in the surface albedo. Although most of the albedo values in this paper refer to clear-sky, local noon values, clear-sky daylight averages could be calculated and the effects due to clouds incorporated.

Albedo measurements are made by instruments placed directly over surfaces or carried by airplanes. For details on instrumentation and techniques the reader is referred to Kuhn and Suomi (1958), Roach (1961), Bauer and Dutton (1962) and Bartman (1967). Aircraft measurements must be made at low altitudes in order to minimize atmospheric effects.

Bauer and Dutton (1962) have demonstrated that albedo measurements up to about 1000 ft are within 5% of the surface value. High-altitude flights (e.g., Roach, 1961) and satellites (e.g., Conover, 1965) produce planetary albedo values and not true surface albedos although inversion techniques have been developed (e.g., Otterman, 1977) to invert surface albedo values.

Posey and Clapp (1964) and Kung *et al.* (1964) have presented surface albedo models for global conditions and North America, respectively. The model developed by Posey and Clapp employed a map of surface characteristics (Bartholomew, 1922) which recognized only six land surface characteristics. The categories did not differentiate between farming and grazing areas, forests of a deciduous or coniferous nature, shrub or sand deserts, nor did the map provide recognition of rain forests, rice growing regions, marshes or irrigated areas. These categories have all been included in this work. Comparing their land use map to a more recent edition of the atlas they used (Bartholomew, 1977) reveals significant differences, especially in the Sahara desert area, central Asia, the tundra reaches of Siberia, and Europe.

Their sources of albedo values were Budyko (1958), Bauer and Dutton (1962), Larsson (1963) and the *Smithsonian Meteorological Tables* (1951). Their seasonal results, especially over land areas in winter, are quite low and do not appear to represent snowcover effects. Over continental areas there is little, if any,

TABLE 1. Latitude and longitude extents, surface area and the number of data points in the data sets NSA, EAF and ASA.

Data set	Latitude extent	Longitude extent	Surface area (km^2)	Number of data points
North and South America	66.67°N–60.28°S	165°–33°W	1.8819×10^8	31 234
Europe and Asia	66.67°N–60.28°S	33°W–80°E	1.3658×10^8	23 280
Asia and Australia	66.67°N–60.28°S	80°E–165°W	1.3089×10^8	22 310

seasonal variation. In spite of these deficiencies it is widely referred to as the source of surface albedo information.

The model of Kung *et al.* (1964) was restricted to North America with good surface differentiation of land features. An extensive flight program over North America (predominantly over the United States) provided the input albedo values. This measurement program provided an excellent collection of values for various surface features as a function of season for cloud-free conditions. Their results include albedo maps for mean, maximum and minimum snowcover and exhibit expected seasonal variations. We make extensive use of their albedo measurements in this work.

2. The model

a. Surface categories selection

The earth's surface was divided into five sections and data on the surface characteristics of each section recorded. The sections were 1) North and South America (NSA), 2) Europe and Africa (EAF), 3) Asia and Australia (ASA), 4) the North Pole and 5) the South Pole. The NSA, EAF and ASA regions extended from 66.67° N to 60.28° S and encircled the globe. The extents of the data sets are detailed in Fig. 1.

Land use data was obtained from land usage maps in the *Oxford 1973 World Atlas* (Cohen, 1973). The maps contained 12 major categories which we further subdivided into 24 land categories, 8 ocean categories and 7 inland water categories to provide more detailed albedo characteristics. Over the Oxford maps a uniform grid of 194 latitude and 396 longitude lines was placed and the dominant surface characteristics of each grid element was read off. A total of 76 824 elements with an average area of 5930 km² comprise the data sets NSA, EAF and ASA.

TABLE 2. Seasonal and latitudinal clear-sky, local-noon surface albedo values for ocean surfaces (from Kondratyev, 1973).

Latitude band	January–March	April–June	July–September	October–December
85°–75°N	50.0	14.7	20.7	50.0
75°–65°N	39.5	9.0	11.7	38.0
65°–55°N	28.7	6.0	7.0	37.7
55°–45°N	15.0	4.7	5.3	19.3
45°–35°N	8.7	4.3	4.3	10.7
35°–25°N	6.3	4.0	4.0	6.7
25°–15°N	5.0	4.0	4.0	5.0
15°–5°N	4.3	4.0	4.0	4.3
5°–0°N	4.0	4.0	4.0	4.0
0°–5°S	4.0	4.0	4.0	4.0
5°–15°S	4.0	4.3	4.3	4.0
15°–25°S	4.0	5.0	5.0	4.0
25°–35°S	4.0	6.7	6.3	4.0
35°–45°S	4.3	10.7	8.7	4.3
45°–55°S	5.3	19.3	18.3	4.7
55°–65°S	7.0	37.7	28.7	6.0
65°–75°S	11.7	38.0	39.5	9.0
75°–85°S	20.7	50.0	50.0	14.7

TABLE 3. Seasonal clear-sky, local-noon surface albedo values for inland water bodies (see text).

Water body	January–March	April–June	July–September	October–December
Black Sea	24.0	6.0	6.0	11.0
Caspian Sea	32.0	6.0	6.0	11.0
Aral Sea	55.0	6.0	6.0	20.0
Great Lakes	55.0	6.0	6.0	20.0
Northern Canada and Siberia lakes	70.0	6.0	6.0	70.0
Central Asia	55.0	6.0	6.0	20.0
Lake Victoria	6.0	6.0	6.0	6.0

Table 1 defines the characteristics of the data sets. The map was based on a modified Gall projection in which a series of cylinders is passed through the globe at several latitude circles. The grid lines are equally spaced along the cylinders. As a result, the spacing on the cylinders of lines of equal latitude spacing is not uniform. Elements at high latitudes represent less global surface area than those at lower latitudes.

The North and South Poles were divided into segments 10° latitude by 10° longitude. (The southernmost latitude band of the North Polar region was 70–66.67°N and the northernmost latitude band of the South Polar region was 70–60.28°S.) For the North Polar region the area was divided into the land area and six seas. The South Polar region consisted of a continental ice cap, ice shelf, pack ice and open water.

The total earth therefore was divided into 77 040 area elements and each area element was assigned one (or more) of 49 fixed categories of surfaces.

b. Seasonal surface clear-sky, local-noon albedo

The average clear-sky, local-noon albedo for each of the 49 fixed categories of surfaces has been obtained for the four quarters of the year, January–March, April–June, July–September and October–December. The model has been developed to present area-weighted albedo averages as a function of season, latitude and longitude. The results are presented as a single albedo value for each 10° latitude and 10° longitude area. Albedo values for areas smaller or larger can be accommodated if desired.

1) WATER SURFACES

The albedo of a plane water surface (for direct beam solar radiation) is a function of the zenith angle X_s and the index of refraction of the water m. From Fresnel's formula the albedo is given by

$$\omega_s(X_s)=50\left[\frac{\sin^2(X_s-r)}{\sin^2(X_s+r)}+\frac{\tan^2(X_s-r)}{\tan^2(X_s+r)}\right],$$

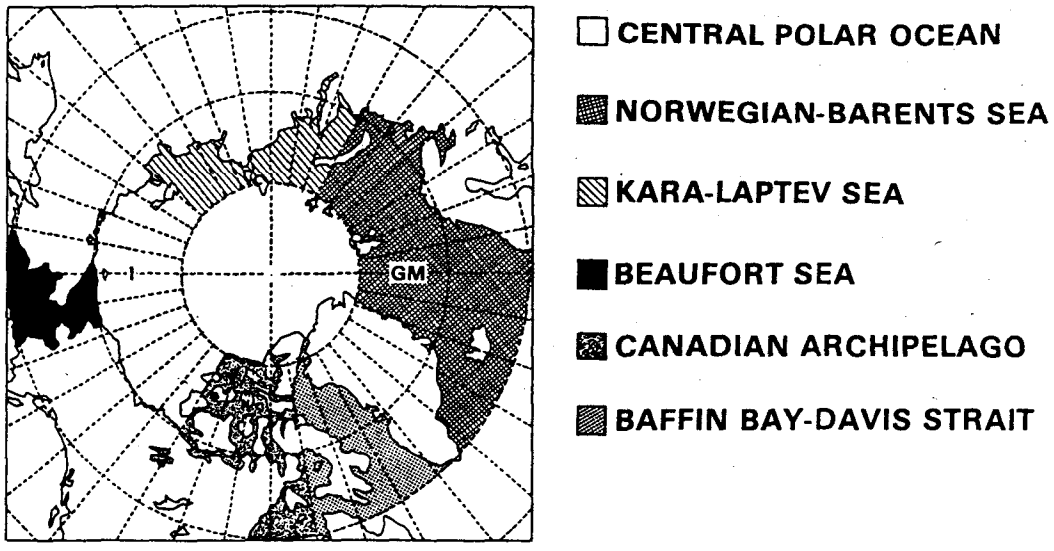

FIG. 2. Water bodies making up the Arctic Ocean (white is land mass).

where the angle of refraction r is found from Snell's law

$$m \sin r = \sin X_s.$$

For normal incidence the previous equation reduces to

$$\omega_s = \left(\frac{m-1}{m+1}\right)^2 \times 100(\%).$$

Unfortunately the application of Fresnel's formula to our work is inappropriate because the albedo of agitated water differs markedly from that of a calm surface. Therefore we have used the measured clear-sky, local-noon surface albedo values for ocean surfaces as a function of northern latitude and season as given by Kondratyev (1973). Although the measurements were made in the Northern Hemisphere they have also been used for the Southern Hemisphere with the appropriate six months seasonal adjustment. The data are presented in Table 2. Budyko (1958) has also presented seasonal and latitudinal water albedo values but his values are valid for cloudy conditions while Kondratyev's results are for cloud-free skies. For zenith angles between 20° to 50° our experimental albedo values agree closely with those obtained for Fresnel's formula.

Also included in the model are seven inland water bodies as listed in Table 3. In the winter some of these bodies freeze. The freezing conditions have been approximated based on climatological information available

TABLE 4. Fractional extent of solid ice (I), pack ice in water (PW) and open water (W) in the Arctic Ocean (Orvig, 1970).

Water body		January–March	April–June	July–September	October–December
Central Polar Ocean	I	0.989	0.989	0.965	0.989
	PW	0.011	0.011	0.035	0.011
	W	0.000	0.000	0.000	0.000
Norwegian Barents Sea	I	0.420	0.383	0.061	0.292
	PW	0.020	0.035	0.087	0.049
	W	0.560	0.582	0.852	0.659
Beaufort Sea	I	0.855	0.855	0.317	0.855
	PW	0.027	0.027	0.187	0.027
	W	0.118	0.118	0.496	0.118
Kara-Laptev Sea	I	0.970	0.970	0.394	0.970
	PW	0.030	0.030	0.193	0.030
	W	0.000	0.000	0.412	0.000
Canadian Archipelago	I	0.970	0.961	0.686	0.966
	PW	0.030	0.039	0.180	0.034
	W	0.000	0.000	0.134	0.000
Baffin Bay-Davis Straits	I	0.524	0.458	0.046	0.258
	PW	0.016	0.034	0.087	0.037
	W	0.460	0.508	0.867	0.705

TABLE 5. Clear-sky, local-noon surface albedo values employed for the Arctic Ocean (Kondratyev, 1973). All values in percent.

	January–March	April–June	July–September	October–December
Solid ice	70	65	60	70
Pack ice in water	55	50	37	55
Open water	45	12	16	44

for each body (Kendrew, 1961; Pincus, 1962; Cohen, 1973). In all cases of partial freezing we assumed that each body can be characterized by a uniform mixture of ice and water over their entire area. When ice conditions exist the albedo values are area weighted using an ice albedo of 65% (Kondratyev, 1973) and open water albedos as given in Table 2.

2) ARCTIC REGION

The Arctic region consists of the surface areas above 66.67°N. It is characterized by an ocean surrounded by land. Following Orvig (1970) the ocean consists of six bodies of water: the central Polar Ocean, the Norwegian-Barents Sea, the Kara-Laptev Sea, the Beaufort Sea, the Canadian Archipelago and Davis Strait-Baffin Bay. The locations of the water bodies are shown in Fig. 2.

The amount of solid ice, pack ice in water and open water in these six water bodies are given by Orvig (1970) and are listed in Table 4. The fractions are assumed uniform throughout each body of water. The albedo values for the solid ice, ice in water and open water are given in Table 5 as taken from Kondratyev (1973). In the Arctic region solid land is found and is covered with tundra and coniferous forests. The albedo values used for these surface types are given in Table 7. In addition, the Greenland ice cap was also considered and given an albedo value of 87% (Orvig, 1970). It should be noted that the extent of solid ice and pack ice represent average estimates over many years. Kukla (1976) has shown that the amount of ice cover is highly variable.

3) ANTARCTIC REGION

The Antarctic region consists of everything south of 60.28°S as shown in Fig. 3. Also shown on the figure are

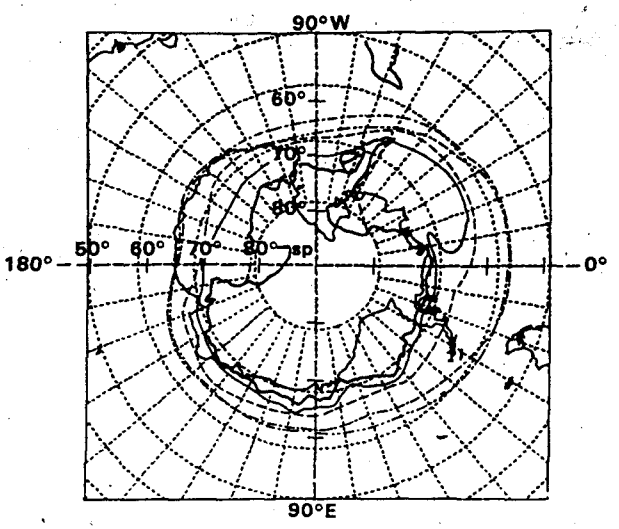

FIG. 3. The extent of pack ice in Antarctic: continent (light lines), permanent ice (dark lines); ice extent: January–March (———), April–June (– – –), July–September (— - —), October–December (— - - —).

the average limits of the pack ice as a function of season, based on results from Fletcher (1968, 1969), Orvig (1970), Kukla (1976) and Cohen (1973). The areal extents of the pack ice are listed in Table 6. The continent, with an area of about 1.4×10^7 km^2, is essentially covered with snow and ice year round and is treated as a permanent ice cap in this work. The pack ice is assumed to consist of ice and water, the fraction changing with season as detailed in Table 6. These fractions were suggested by results summarized by Kukla (1976). As with the Arctic, we assume a uniform mixture of ice and water in the region of the ice pack. The clear-sky, local-noon albedo values are also given in Table 6 as obtained from the measurements of Orvig (1970) and Kondratyev (1973).

4) LAND CATEGORIES

Table 7 lists the categories employed, the surface area covered and the albedo values assigned to them. In all cases, the albedo values refer to Northern Hemisphere seasonal conditions. However the values were used for the Southern Hemisphere by shifting the season by six months.

TABLE 6. Antarctic parameters.

	Average area of the pack ice (10^6 km^2)	Fractions of ice and water in the pack ice		Albedo values (percent)		
				Continental ice cap	Pack ice	Open water
		Ice	Water			
January–March	4.57	0.50	0.50	82	37	16
April–June	8.87	0.75	0.25	82	55	44
July–September	16.13	0.75	0.25	88	55	45
October–December	14.80	0.75	0.25	88	50	12

TABLE 7. Surface categories, surface area covered and seasonal (Northern Hemisphere) albedo values.

Surface category	Surface area (km^2)	Percent of total surface area	Albedo (%) January–March	April–June	July–September	October–December
Arable land with intensive farming						
snow in winter	5.237×10^6	1.026	50.0	16.0	15.0	27.0
no winter snow	1.598×10^7	3.129	14.0	16.0	15.0	14.0
Grazing and marginal farming lands						
snow in winter	5.488×10^6	1.075	50.0	18.0	16.0	20.0
heavy snow in winter	3.804×10^5	0.074	50.0	38.6	16.0	20.0
no winter snow	2.520×10^7	4.935	20.0	16.0	18.0	20.0
Rice lands or regions where paddies dominate	2.633×10^6	0.516	12.0	12.0	12.0	12.0
Other irrigated land in dry areas where paddies do not dominate						
snow in winter and fall	1.687×10^5	0.033	50.0	39.0	17.0	32.0
snow in winter	2.008×10^5	0.039	50.0	17.0	17.0	26.0
no winter snow	1.246×10^6	0.244	20.0	20.0	20.0	20.0
Coniferous forests						
heavy snow areas	1.019×10^7	1.995	47.0	47.0	14.0	47.0
snow in winter	2.625×10^6	0.514	36.0	16.0	14.0	11.0
no winter snow	4.197×10^5	0.082	16.0	16.0	14.0	11.0
Deciduous forest						
snow in winter	3.508×10^5	0.069	33.0	14.0	14.0	19.0
no winter snow	4.654×10^6	0.911	19.0	14.0	14.0	19.0
Mixed coniferous and deciduous forests						
snow in winter	2.025×10^6	0.397	34.5	15.0	15.0	19.0
no winter snow	2.117×10^6	0.415	15.0	15.0	15.0	15.0
Tropical woodlands and grasslands	6.641×10^6	1.300	16.0	16.0	16.0	16.0
Equatorial (rain) forests	1.513×10^7	2.962	7.0	7.0	7.0	7.0
Deserts						
shrubland with winter snows	7.591×10^4	0.015	36.0	22.0	22.0	22.0
shrubland with no winter snow	1.447×10^7	2.833	22.0	22.0	22.0	22.0
sand	4.769×10^6	0.934	42.0	42.0	42.0	42.0
Marshes						
snow in winter	8.494×10^5	0.166	55.0	34.5	14.0	55.0
no winter snow	1.951×10^6	0.382	10.0	10.0	10.0	10.0
Tundra	1.172×10^7	2.295	82.0	82.0	17.0	82.0
Total	1.345×10^8	26.34				

Our agricultural characterization includes arable and mixed farming land where the farming is considered to be the dominant activity, either grazing land and farmland of a marginal quality, rice lands where paddies are the dominant feature, or other irrigated lands in dry areas where paddies are not dominant. Some of the subclassifications have been made simply to provide differentiation between winter snow-covered regions and those which are snow-free.

Kung *et al.* (1964) presented numerous clear-sky, local-noon surface albedo measurements for regions of the United States for different seasons. The albedo values for arable land with intensive farming, grazing and marginal farming lands categories represent the average of all of measured values and agree well with values presented by Budyko (1958), Bauer and Dutton (1962), Sellers (1965) and Kondratyev (1969, 1973). For those regions denoted as having no winter snow the January–March and October–December values imply that the fields are in a fallow, plowed or immature state. As shown in Table 7, the arable land category was broken down into snow and snow-free subclassifications while the grazing and marginal farm land category was divided into three categories: areas with heavy snow such as Siberia and Tibet, areas with winter snow and snow-free areas.

The albedo value for rice lands and paddies is taken from Kondratyev (1969). Unfortunately, seasonal results were not given but they would not be expected to vary greatly with season.

The irrigated land was subdivided to include areas in California, South America, the Mediterranean,

Middle East, central Asia where winter snows are absent, Siberian locations where snow is found in the winter and fall, and other locations where only winter snows are found. The albedo values represent averages of the values presented by Kung *et al.* (1964) and Kondratyev (1973).

Our five forest categories include 1) coniferous, 2) deciduous, 3) mixed coniferous and deciduous, 4) tropical woodlands and grasslands and 5) equatorial forests. The coniferous, deciduous and mixed coniferous and deciduous forest categories were subdivided to distinguish between snow-covered and snow-free areas. The coniferous forest category includes the high-latitude forests in Canada and Europe, where the snow cover lasts about nine months, midlatitude forests with only winter snows, and forests where no snow is found.

The albedo values for high latitude coniferous forests represent an average of the measurements by Kung *et al.* (1964) and Kondratyev (1973). The two sources were in close agreement, differing by no more than a percentage point or two. The midlatitude values are the average of extensive measurements by Kung *et al.* (1964).

The deciduous forest values are based on the measurements of Kung *et al.* (1964) from a variety of trees and locations. Their values agree well with values presented by Bauer and Dutton (1956), Budyko (1958) and Kondratyev (1969). The mixed coniferous and deciduous forests category assumes an equal mixture of the two and the albedo values are the average of their individual values.

The tropical woodlands and grasslands and equatorial forests are all found between the latitudes 25°N and 20°S. Kung *et al.* (1964) gave a season independent albedo value of 16% for the tropical woodlands and grasslands. This value is in the range of values suggested by the *Smithsonian Meteorological Tables* (1951), Budyko (1958), Sellers (1965), Kondratyev (1969) and the recent satellite inferred results of Rockwood and Cox (1978). For equatorial forests we use the value of 7% given in the *Smithsonian Meteorological Tables* (1951) with no seasonal dependence.

The deserts are considered to be shrubland or sand types, the shrubland type dominating. In the shrubland

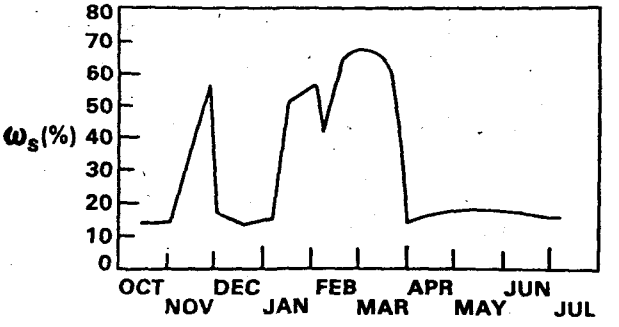

FIG. 4. Surface albedo as a function of month for a section of Wisconsin (Bauer and Dutton, 1962).

category deserts in the interior of Asia (Gobic and Turkestan) and in the intermountain zones of North America can experience winter snow. Hence the albedo values assigned are season-dependent. The albedo values for both the shrubland desert subclassifications are based on the measurements of Kung *et al.* (1964) as well as other values reported by Budyko (1958) and Sellers (1965). The sand desert values are based on values reported by Otterman (1977) and Rockwood and Cox (1978).

The marshes and bogs were broken down to include those that may be snow covered (those in northern Canada and Siberia) and those that are not. The values assumed are based on the results of Kung *et al.* (1964), Kondratyev (1973) and Rockwood and Cox (1978).

In common usage, tundra areas can refer to a region characterized by sparse vegetation such as mosses, lichens, grasses or low shrubs. Tundra regions may also be defined according to climatological variables. In this case, it is a high-altitude region with very low winter temperatures, average summer temperatures less than 50°F, generally strong winds and low precipitation. We use a definition that encompasses both climatic and vegative descriptions. Geographic areas characterized as tundra are found in the Arctic regions, central Asia, the Rocky Mountains and the Andes Mountains. The surface albedo values assumed are the average of measurements presented by Kung *et al.* (1964) and Kondratyev (1973) both of which were in very close agreement.

TABLE 8. Average seasonal extent of snow and ice in the Northern Hemisphere in 10^6 km^2 (after Kukla, 1976).

	1967	1968	1969	1970	1971	1972	1973	1974	1975
January–March	—	58.73	55.90	53.23	58.27	59.83	59.10	57.07	57.30
April–June	29.67	30.20	31.17	29.83	32.47	32.80	32.83	34.43	31.80
July–September	13.13	11.93	11.40	11.27	14.27	13.37	12.77	12.47	11.93
October–December	33.40	35.0	36.23	37.57	41.80	45.87	41.77	39.73	39.90

	Average	Model results	Percent difference
January–March	57.43	52.78	−8.10
April–June	31.69	35.64	12.46
July–September	12.50	10.72	−14.24
October–December	39.03	38.81	−0.56

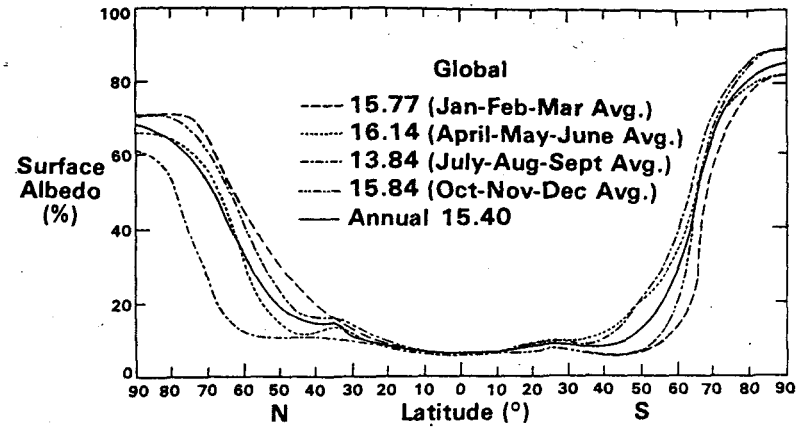

FIG. 5. Clear-sky, local-noon surface albedo versus latitude obtained in this work.

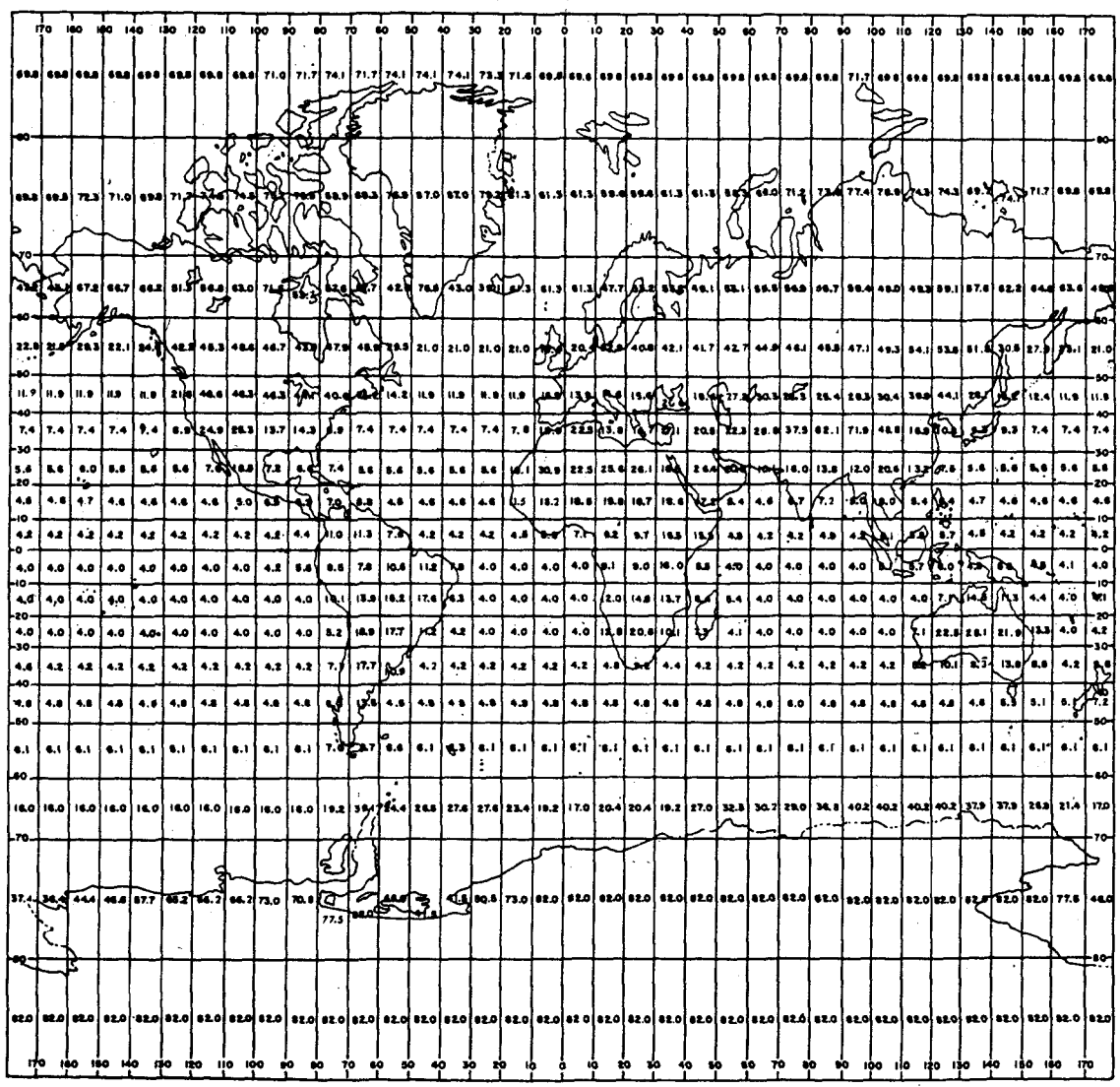

FIG. 6. Surface albedo map for January–March.

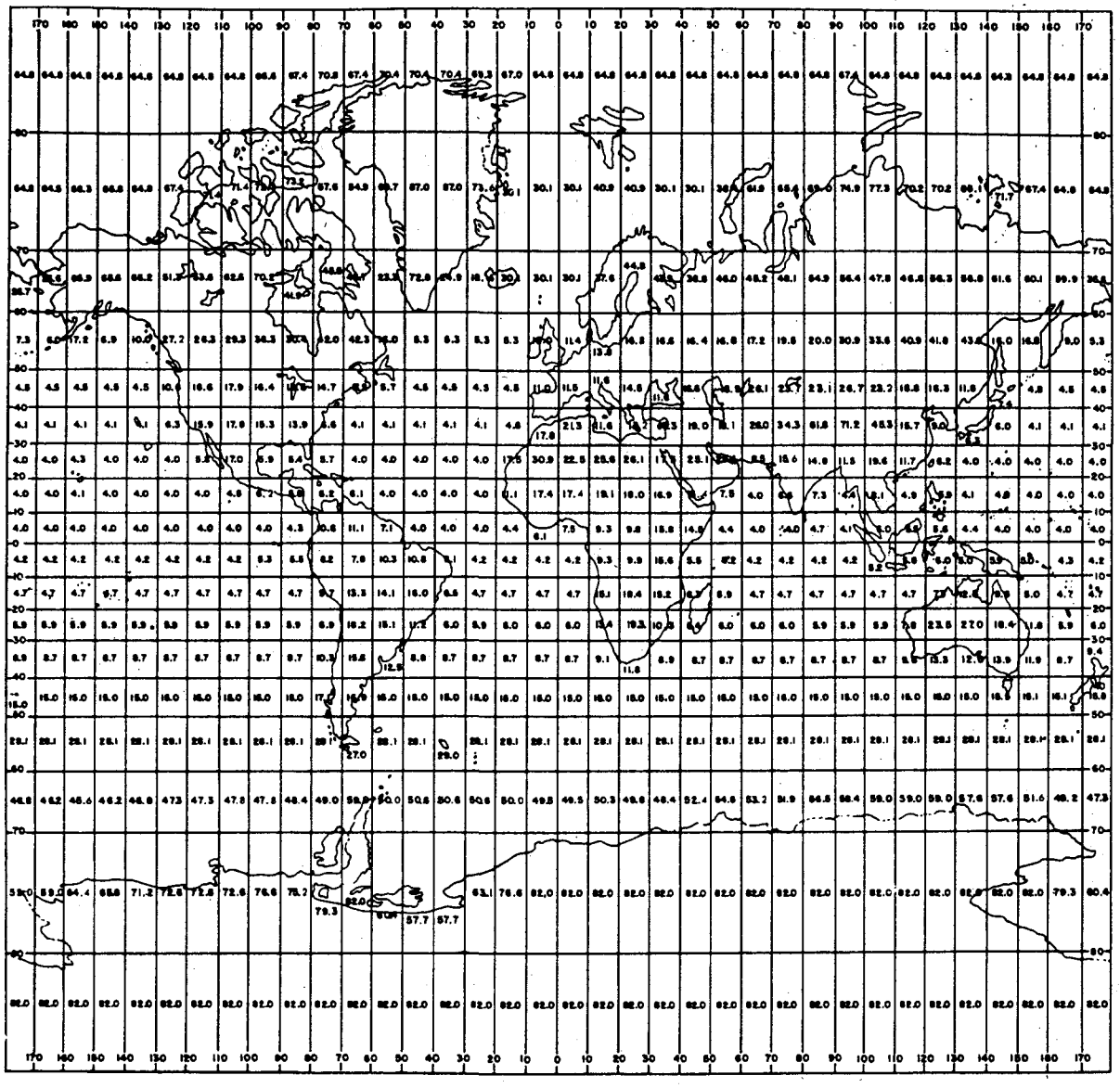

FIG. 7. Surface albedo map for April–June.

During the winter months the surface albedo increases greatly as a result of snow cover. Fig. 4 shows the average albedo values measured over a portion of Wisconsin as a function of season, based on results presented by Bauer and Dutton (1962). As Fig. 4 shows, the seasonal variation in surface albedo can be considerable. The more ground covered by snow the higher the measured albedo value. Also the surface albedo increases with snow depth up to about 5 inches (12.70 cm) at which time the albedo is unaffected by any further increases (Kung *et al.* 1964). The albedo increase is greatest from snow depths of 0–1 inch. Another factor besides depth is the condition of the snow. Freshly fallen snow can have a measured surface albedo as high as 88% while older snow can have values of 75% and less (Kondratyev, 1973). The crystalline nature is also important (Bohren and Barkstrom, 1974; Kondratyev, 1973). The larger the snow grain the less the albedo.

Clearly, then, it is important to know and include the extent of snow cover on the earth's surface. For the United States we adopted the procedure of Kung *et al.* (1964) and let those regions with an average wintertime snow depth of 1 inch or more (U.S. Army Corps of Engineers, 1954; Kendrew 1961; Cohen, 1973; Bryson and Hare, 1974) define the conditions of snow-covered surfaces. In South America, only the Andes and Tierra del Feuge were assumed to experience consistent snow in winter (Kendrew, 1961; Cohen 1973). Winter snow

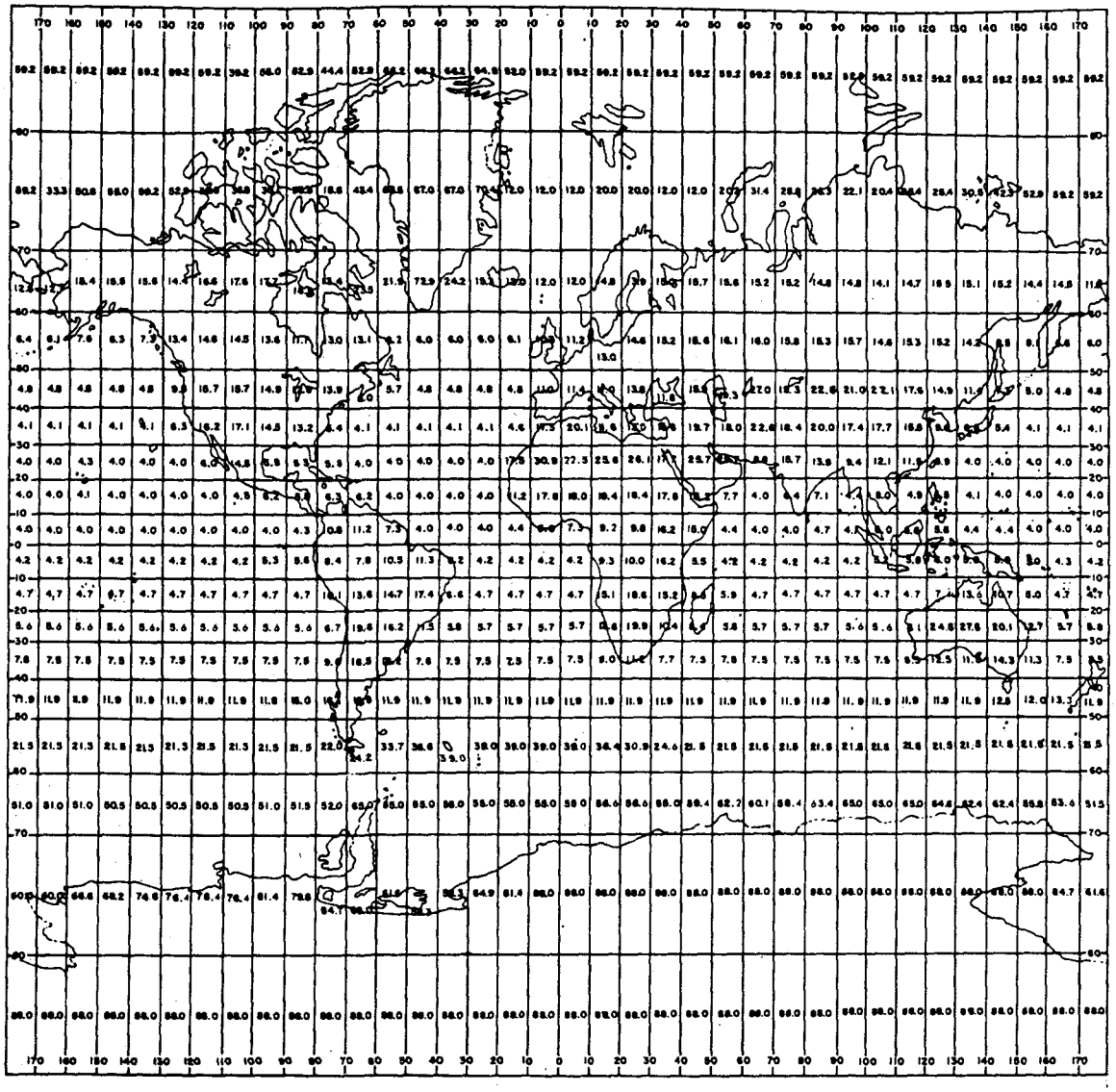

FIG. 8. Surface albedo map for July–September.

in Europe consists of those regions that have more than 40 days of snow per year following Kendrew (1961), Wallen (1970) and Cohen (1973). In Asia, snow-covered surfaces were defined from the results of Kendrew (1961), Wallen (1970), Cohen (1973) and Lackwood (1974). Kukla (1976) has presented results for the average seasonal extent of snow and ice in the Northern Hemisphere which is reproduced in Table 8. If we compare our extent of snow and ice coverage with Kukla's results, our January–March, July–September and October–December results are low while the April–June results are high. Kukla (1976) estimates that his results are correct to within 5–7%.

3. Discussion of results

Fig. 5 displays the average clear-sky, local noon latitudinal surface albedo values and the global averages for the four quarters of the year, January–March, April–June, July–September and October–December. The global average values are the area-weighted latitudinal values and include the fact that portions of the polar regions are not illuminated during their respective fall and winter. Figs. 6–10 are maps of surface albedo for 10° latitude by 10° longitude elements for each quarter and the annual case. Expected seasonal variations and geographical effects are evident. As the polar ice caps and snowlines recede in the spring hemisphere

the high-latitude albedo values diminish. The predominance of ocean surfaces in the low latitudes produces the low-albedo values found there. The slight seasonal variation in low-latitude water albedo values (see Table 2) is also evident as well as the slight increase in albedo in the latitudinal band between 30–40°N. This increase is due to the tundra regions of Tibet and the central Asian deserts. The high-albedo values of the tundra for the January–March, April–June and October–December periods (82%) result in the Tibetan tundra being the largest single contributor to the area-weighted albedo in this latitude band. In the 10–30°S latitude bands, another slight increase resulting from the South American and Australian land masses is evident.

Posey and Clapp (1964) did not publish latitudinal or global average values from their model but Shutz and Gates (1972, 1973, 1974) have compiled the Posey and Clapp data onto a 4° latitude by 5° longitude grid and determined latitudinal and seasonal averages for April, July and October. The global values they give are, respectively, 17.4, 14.0 and 15.4% and do not include the fractional illumination in the polar regions. Their June–August plot is shown compared with our July–September results in Fig. 11. The major differences lie in the polar regions. In the Antarctic, Posey and Clapp (1964) do not consider the seasonal variations in the pack ice with the detail used in this work. The albedo value they assign for Antarctic snow cover (80%) is seasonally independent and less than the seasonally dependent values used in this work. During April and October the north polar results of Posey and Clapp (1964) are consistently higher than ours. The source of their ice extent data is not clear nor the degree of sea-

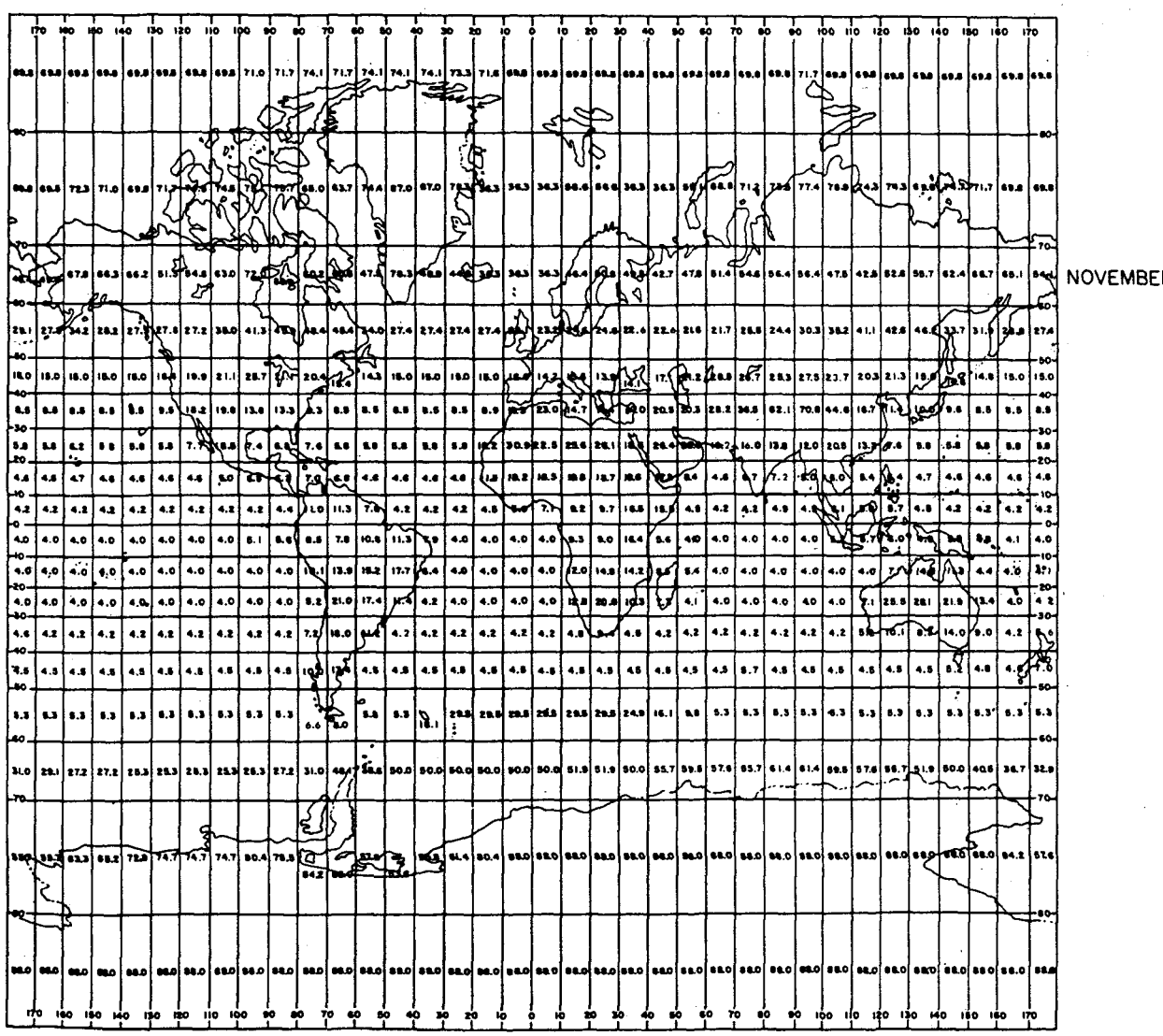

FIG. 9. Surface albedo map for October–December.

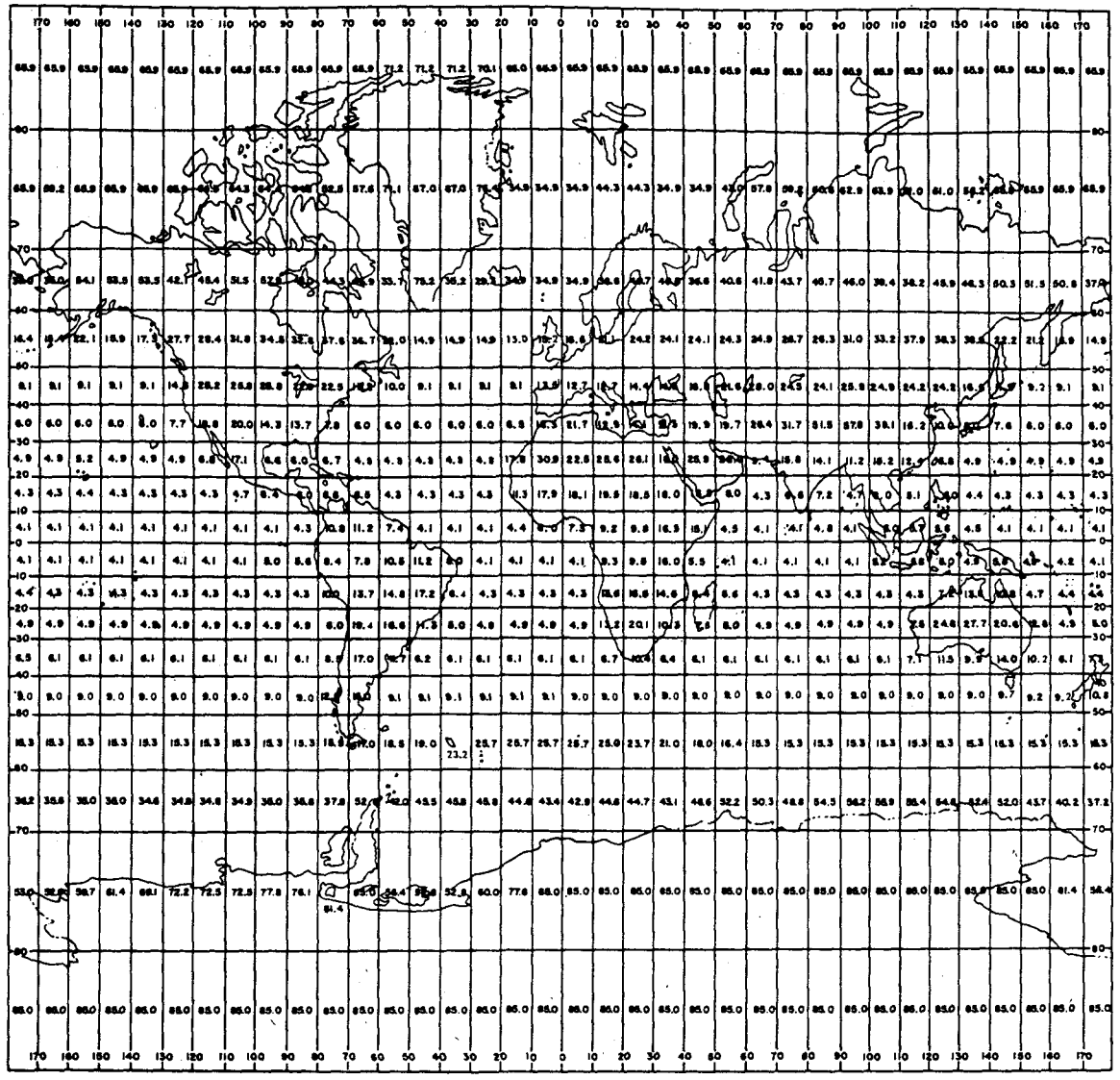

FIG. 10. Surface albedo map for annual conditions.

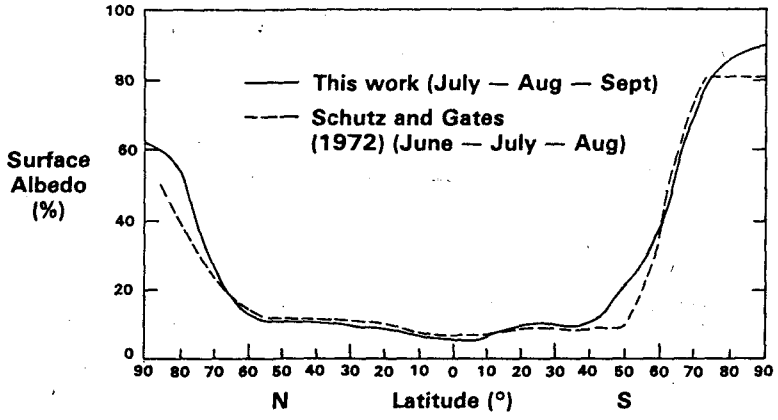

FIG. 11. Comparison of latitudinally averaged surface albedo values from this work for July–September and Schutz and Gates (1972) for June–August.

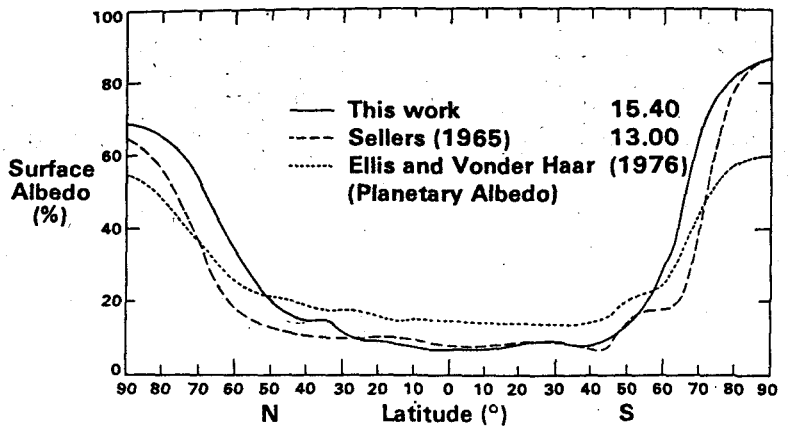

FIG. 12. Comparison of annual, latitudinal surface albedo results of Sellers (1965) and this work. The planetary albedo results of Ellis and Vonder Haar (1976) are shown, also. Clear-sky, local-noon surface albedo versus latitude curves from three different works.

sonal variation. The Arctic data used in this work include a breakdown of the Arctic Ocean into six component bodies of water with separate solid ice, pack ice and open water fractions. In low latitudes, Posey and Clapp (1964) employed water albedo values consistently larger than ours. Hence, in low latitudes their latitudinal results are larger than ours. Further comments on the effects of the water albedo differences will be made later.

In Fig. 12 we compare our annual latitudinal and global surface albedo values with those of Sellers (1965) and the planetary albedo results of Ellis and Vonder Haar (1976). Sellers' values are based primarily on the work of Houghton (1954) which used much larger area elements and fewer albedo subdivisions than used in this work. The results of Ellis and Vonder Haar (1976) are based on cloud-free measurements from Nimbus 3. At low latitudes there is good agreement between Sellers' (1965) data and our model.

In midlatitudes, the agreement breaks down, due primarily to the coarser grid and surface differentiation used in the Houghton (1954) model. The planetary albedo results of Ellis and Vonder Haar (1976) demonstrate that a high surface albedo value does not necessarily result in a high planetary albedo. The planetary albedo is the albedo of the combined earth–atmosphere system. Over surfaces with low surface albedo values, the planetary albedo increases with height because of the addition of Rayleigh scattering. There is absorption of the reflected beam occurring, but the added Rayleigh scattering component exceeds the amount depleted by absorption. Over surfaces with high surface albedos, the reverse is true. The amount of atmospheric absorption of the reflected beam exceeds the added Rayleigh

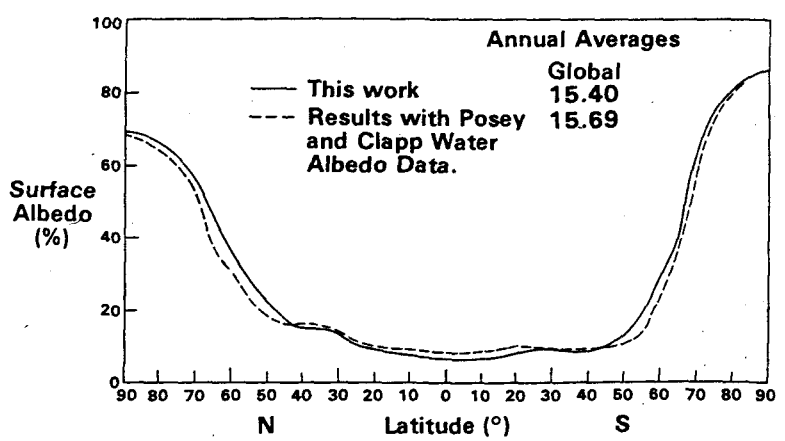

FIG. 13. Clear-sky, local-noon surface albedo versus latitude curves for annual conditions for this work and with Posey and Clapp water albedo substituted.

TABLE 9. Seasonal and latitudinal surface albedo values for water surfaces used by Posey and Clapp (1964). The values in parentheses are those used in this work. All values are in percent.

Latitude band	January–March	April–June	July–September	October–December
65–85° N	10.0 (43.0)	12.0 (10.1)	10.0 (14.7)	24.0 (42.2)
55–65° N	8.5 (28.7)	8.5 (6.0)	11.0 (7.0)	15.5 (37.7)
45–55° N	7.5 (15.0)	7.5 (4.7)	11.0 (5.3)	16.0 (19.3)
35–45° N	6.5 (8.7)	7.0 (4.3)	8.5 (4.3)	11.0 (10.7)
25–35° N	6.0 (6.3)	6.0 (4.0)	7.5 (4.0)	9.0 (6.7)
15–25° N	6.0 (5.0)	6.0 (4.0)	6.5 (4.0)	7.5 (5.0)
5–15° N	6.0 (4.3)	6.0 (4.0)	6.0 (4.0)	6.5 (4.3)
0–5° N	6.0 (4.0)	6.0 (4.0)	6.0 (4.0)	6.5 (4.0)
5–0° S	6.0 (4.0)	6.5 (4.0)	6.0 (4.0)	6.0 (4.0)
15–5° S	6.0 (4.0)	6.5 (4.3)	6.0 (4.3)	6.0 (4.0)
25–15° S	6.5 (4.0)	7.5 (5.0)	6.0 (5.0)	6.0 (4.0)
35–25° S	7.5 (4.0)	9.0 (6.7)	6.0 (6.3)	6.0 (4.0)
45–35° S	8.5 (4.3)	11.0 (10.7)	6.5 (8.7)	7.0 (4.3)
55–45° S	11.0 (5.3)	16.0 (19.3)	7.5 (18.8)	7.5 (4.7)
65–55° S	11.0 (7.0)	15.5 (37.7)	8.5 (28.7)	8.5 (6.0)
85–65° S	10.0 (14.7)	24.0 (42.2)	10.0 (43.0)	12.0 (10.1)

scattering component. As a result, the planetary albedo is less than the surface albedo.

Water, being the largest surface feature on the earth, has a large impact on global albedo. We shall present results utilizing the water albedo values of Posey and Clapp (1964), which are outlined in Table 9. In parentheses are the values used in this work. The values used by Posey and Clapp were based on measurements made on cloudy days while those used in this work are for cloud-free skies. As shown in Table 9, there is considerable difference between the values. The Posey and Clapp data are high in the low latitudes and for May and August in the high latitudes. Their data also do not exhibit the expected seasonal variation, higher values in winter and fall when the solar zenith angle is large. Their high-latitude fall and winter values are too low and do not agree well with published results (e.g. Kondratyev, 1973). Payne (1972) has also published ocean surface albedo values for various clear and cloudy sky conditions. While agreeing with Budyko's results for latitudes to 40°, there are large discrepancies at higher latitudes. In Fig. 13 we compare the annual latitudinal surface albedo results using the water albedo values of Posey and Clapp with the results of our model. The global annual results are also given. In high latitudes the surface albedo values with the Posey and Clapp data are slightly less while in the middle to low latitudes they are large. In this region the contribution of water surfaces to any area-weighted average is greatest and as a result the global annual surface albedo is larger with the Posey and Clapp water albedo data.

4. Summary

1) A 77 040 area element surface albedo model was developed which permits consideration of seasonal and latitudinal variations in 49 area-type categories.

2) The greatest inaccuracies in previously reported models were found to be due to (i) omitted seasonal variations in snow and ice covers, (ii) disregard of the latitudinal variations in the surface albedo of the agitated ocean surface water, and (iii) lack of detail of surface characterization.

3) The present model can be adapted to study changes in surface albedo with changes in climatic conditions, e.g., an approaching ice age.

4) The model was used to calculate improved seasonal and annual-average values of surface albedo for each 10° latitudinal band. The annual global average albedo was calculated to be 15.4% as compared to 13.0% for previous predictions.

REFERENCES

Bartholomew, J. G., Ed., 1922: *The Times Atlas and Gazetteer of the World.* The Times Printing House Square, London, 258 pp.

——, Ed., 1977: *Mini Pocket Atlas.* John Bartholomew and Son, Ltd., Edinburgh, 160 pp.

Bartman, F. L., 1967: The reflectance and scattering of solar radiation by the earth. University of Michigan, 05863-11-T.

Bauer, K. G., and J. A. Dutton, 1962: Albedo variations measured from an airplane over several types of surface. *J. Geophys. Res.*, **67**, 2367–2376.

Bohren, C. F., and B. R. Barkstrom, 1974: Theory of the optical properties of snow. *J. Geophys. Res.*, **79**, 4527–4535.

Bryson, R. A., and F. K. Hare, 1974: *Climates of North America.* Vol. 2, *World Survey of Climatology*, Elsevier, 420 pp.

Budyko, M. I., 1958: *The Heat Balance of the Earth's Surface.* Translated by Nina A. Stepanova, Office of Climatology, U.S. Weather Bureau, 259 pp.

Cohen, S. B., Ed., 1973: *The Oxford World Atlas.* Oxford University Press, 190 pp.

Conover, J. H., 1965: Cloud and terrestrial albedo determinations from TIROS satellite picture. *J. Appl. Meteor.*, 4, 378–386.

Ellis, J., and T. H. Vonder Haar, 1976: Zonal average earth radiation budget measurements from satellites for climate studies. Atmos. Sci. Pap. 240, Colorado State University, 50 pp.

Fletcher, J. O., 1968: The polar oceans and world climate. P-3801, The RAND Corporation, Santa Monica, CA.

——, 1969: The influence of variable sea ice on thermal forcing of global circulation. P-4175. The RAND Corporation, Santa Monica, CA.

Houghton, H. G., 1954: On the annual heat balance of the Northern Hemisphere. *J. Meteor.*, 11, 1–9.

Idso, S. B., R. D. Jackson, R. J. Reginate, B. A. Kimball and F. S. Nakayama, 1975: The dependence of bare soil albedo on soil water content. *J. Appl. Meteor.*, 14, 109–113.

Kendrew, W. G., 1961: *The Climates of the Continents.* Oxford University Press, 608 pp.

Kondratyev, K. Ya., 1969: *Radiation in the Atmosphere.* Academic Press, 912 pp.

——, 1973: *Radiation Characteristics of the Atmosphere and the Earth's Surface.* Amerind Pub. Co., New Delhi, 580 pp.

Kuhn, P. M., and V. E. Suomi, 1958: Airborne observations of albedo with a beam reflector. *J. Meteor.*, 15, 172–174.

Kukla, G. J., 1976: Global variation of snow and ice extent. Paper presented at COSPAR.

Kung, E. C., R. A. Bryson and D. H. Lenschow, 1964: Study of a continental surface albedo on the basis of flight measurements and structure of the earth's surface cover over North America. *Mon. Wea. Rev.*, **92**, 543–564.

Lackwood, J. G., 1974: *World Climatology: An Environmental Approach.* St. Martin's Press, New York, 330 pp.

Larsson, P., 1963: The distribution of albedo over Arctic surfaces. *Geograph. Rev.*, 53, 572–579.

Lian, M. S., and R. D. Cess, 1977: Energy balance climate models: A reappraisal of ice-albedo feedback. *J. Atmos. Sci.*, 34, 1058–1062.

Orvig, S., Ed., 1970: *Climates of the Polar Regions.* Vol. 14, *World Survey of Climatology*, Elsevier, 370 pp.

Otterman, J., 1977: Monitoring surface albedo change with LANDSAT. *Geophys. Res. Lett.*, 4, 441–444.

Paltridge, G. W., and C. M. R. Platt, 1976: *Radiative Processes in Meteorology and Climatology.* Elsevier, 318 pp.

Payne, R. E., 1972: Albedo of the Sea Surface *J. Atmos. Sci.*, 29, 959–970.

Pincus, H. J., Ed., 1962: Great Lakes basin. AAAS Publ. No. 71, Washington, DC.

Posey, J. W., and P. F. Clapp, 1964: Global distribution of normal surface albedo. *Geofis. Int.*, 4, 33–48.

Reck, R. A., 1978: Response of calculated radiative-convective temperature profile to variations in model physical parameters: Uncertainty in the calculated temperature from input data error. General Motors Res. Lab., GMR-2612, Warren, MI, 17 pp.

Roach, W. T., 1961: Some aircraft observations of fluxes of solar radiation in the atmosphere. *Quart. J. Roy. Meteor. Soc.*, 87, 346–363.

Rockwood, A. A., and S. K. Cox, 1978: Satellite inferred surface albedo over northwestern Africa. *J. Atmos. Sci.*, 35, 513–522.

Schutz, C., and W. L. Gates, 1972: Global climatic data for surface, 800 mb, 400 mb: July. R-1029-ARPA, 180 pp.

——, and ——, 1973: Global climatic data for surface, 800 mb, 400 mb: April. R-1317-ARPA, 192 pp.

——, and ——, 1974: Global climatic data for surface, 800 mb, 400 mb: October. R-1425-ARPA, 192 pp.

Sellers, W. D., 1965: *Physical Climatology.* The University of Chicago Press, 272 pp.

Smithsonian Meteorological Tables, 1951: Smithsonian Institution, Washington, DC, R. J. List, Ed., 527 pp.

U.S. Army Corps of Engineers, 1954: Depths of snow cover in the northern hemisphere. Arctic Construction and Frost Effect Laboratory, New England Division, Boston.

Wallen, C. C., Ed., 1970: *Climates of Northern and Western Europe.* Vol. 5, *World Survey of Climatology*, Elsevier, 252 pp.